Industrial Engineering Journal
ISSN: 0970-2555
Volume : 52, Issue 10, No. 3, October : 2023

MICROPOLAR FLOW THROUGH A STRETCHED SURFACE WITH SECOND-ORDER SLIP IN THE BOUNDARY LAYER AND HEAT TRANSFER

[1]B. Saidulu ,[2]K. Sreeram Reddy and [3]M. Sathyanarayana Department of Mathematics, University College of Science, Osmania University, Hyderabad, Telangana,
Email: [1]bandhamssaidulu@gmail.com, [2]dr_sreeram_reddy@yahoo.com,
[3]manthrisathyam926@gmail.com

Abstract
Its objective in this paper would be to investigate the effects of a magnetic field and a second-order slip flow just on boundary layer flow for a micropolar fluid that would be moving through a stretching sheet. All these basic non-linear boundary-value problems have been made easier to understand by putting them into a single linked higher-order non-linear ordinary differential equation with non-dimensional parameters. Following that, a mathematical formulation for velocity, microrotation, and temperature was achieved. These problems were solved numerically by utilising the method bvp4c provided by MATLAB. Such results were obtained through a variety of governing variables. The effect of key parameters on the microrotations, temperature, concentration, skin friction coefficient, local Nusselt number and velocities were all examined in relation to certain numerical estimates. According to observations, the slip parameter γ numbers should be increased in order to see a significant increase in the skin friction coefficient CF. This study between earlier investigations that are found within the body of published research was carried out, and the results show a great correlation.

Keywords: MATLAB, bvp4c, Micropolar fluid, Temperature.

Nomenclature

u, v	$x, y-$Components of velocity	j	microinertia per unit mass (N/kg)
μ	Dynamic viscosity$(kg\ m/s)$	c_p	specific heat at constant pressure $(J/Kg\ K)$
ρ	Density of the fluid(kg/m^3)	C_f	Skin friction coefficient
δ	second-order slip factor	g	Non-Dimensional microrotation
γ	1st-order slip factor	θ	Non-Dimensional Temperature
υ	kinematic viscosity(m^2/s)	Pr	Prandtl number
ɳ	similarity variable	K_n	Knudsen number
u_w	surface velocity(m/s)	λ	open channel for molecule
n	n microrotation parameter	α	the momentum accommodation coefficient
f'	Dimensionless velocity	Ω	Spin gradient velocity vector
C_w	concentration of the fluid at the surface	T	temperature inside the boundary layer

INTRODUCTION

As a result, how a hydromagnetic stream flows in its stretching sheet, including how temperature continues to move through it, has significant industrial significance, and there have been numerous publications and analyses dealing with this topic throughout the previous investigation. If polymerization occurs in beverages, meals, and even sludge, this plays a significant role in the creation of chemical manufacturing substances.

The fundamental assumptions of the Navier-Stokes theory are defined in the process of no-slip flow conditions. However, there are a few instances where a similar requirement would be inappropriate. Because polymeric melting frequently displays microscopic boundary slip, which is

typically controlled by a non-linear but monotone connection between the slip velocity and the suction, the no-slip criterion is particularly unsuitable for the majority of non-Newtonian fluids. Solutions for the fluids that show boundary slip include cleaning heart implants for vestibular chambers. A slip boundary condition in measures about shear stress was proposed by Navier [1]. In order to solve the complete Navier-Stokes solutions, where magnetic materials circulate across a stretched surface, Andersson [2] developed a sealed structure approach. Fang et al. [3] gave another exact analytical expression of MHD flow across a porous, stretched surface with slip boundary conditions. Bhattacharyya et al. [4] looked at a flow that was not steady across sheets that were stretched and had slip boundary conditions. Furth more, MHD Ahmad et al. [5] examined the Newtonian liquid motion beyond a decreasing surface according to a temperature slip. Additionally, Yang et al. [6] had suggested the second-order slip theory by the flow of heat exchange through a dual Maxwell fluid. Sahoo [7] looked into how heat moves and flows as a third fluid in a partially slip boundary condition. Das [8] investigated how heat production while absorbing, thermal buoyancy, and partial slip affected the circulation of current nanofluids through a porous stretched sheet. Another phenomenon involving heat transmission inside every wake of second-order slip effects beside a continuously extending surface was suggested by Majeed et al. [9]. Nonlinear 2nd array slide circulation including heated transmission across a flexible shrinking surface were proposed by Singh and Chamkha [10]. Roşca, A. V., & Pop, I [11] research on a transparent shrinking surface immersed in a permeable layer by a second-order slip is extended within the current study to the situation of a fluid over a shrinking surface, where dual responses are possible.

Theoretical research involving the transfer of heat along with mass in an MHD turbulent fluid, including temperature and velocity first-order slip across a stretched surface under various boundary temperatures, was conducted by Turkyilmazoglu [12]. The constant compressible flow across different geometries that had first together with second-order slip was solved similarly by Zhang et al. [13]. Varying slip boundary circumstances' effects on stress non-Newtonian fluid motion were investigated by Pereira [14]. Through the use of stretched sheets, Akyildiz et al. [15] looked into presence outcomes and 3rd-order non-linear finite difference issues. The rate of heat transfer for the slip flow of fluids through a horizontal plane within the permeable medium under uniform heat flux conservation equations has been studied by Yazdi et al. [16]. Thompson and Troian [17] presented a global regressive boundary condition for slips that takes into account the dynamic characteristics of either the slip duration or the usual areas of significant subsurface shearing. Therefore, Noghrehabadi et al. [18] comprehensive explanation about the impact of partial slip-on boundary layer flow along with the transmission of nanoparticles through stretched sheeting under stable wall temperature was provided. Second-order slip circulation and heat transfer through a stretched surface were investigated by Mahantesh et al. [19]. Chauhan and Olkha [20] have looked at the global temperature flux while looking at the slip flow of second-grade fluid through stretched sheets inside a permeable material. With the process of solving the Navier-Stokes problem involving second-order slip flow through a porous stretched surface, Aziz [21] achieved accurate answers. These implications for slip effects on stretching circulation involving conductive dissipation were discussed by Qasim et al. [22]. saidulu. B et al. [23-25] micropolar free convective fluid flow over a stretched porosity sheet with flow rate within a systematic investigation of the influence of radioactivity on thermal transfer and mass transport. The radiative impact over the hybrid convective boundary surface circulation of an extremely thick viscosity including expansion over a flat channel having homogeneous heat transfer was studied by Hossain and Takhar [26]. Pantokratoras [27] investigated magnetohydrodynamic boundary surface flow across a heated stretched surface with changing viscosity numerically. The electric force is important because the hollow's thermal transmission mechanism thus functions as a natural thermal source. Kalaivanan et al. [28] looked at how an angled electric force affected the slip flow of viscoelastic fluid across a stretched surface. With each mixed slip, electromagnetic and molecular diffusion factors have one practical approach here to magnetohydrodynamic slip flow that was discovered by Fang et al. [29] in their study. Bakr[30] has spoken about how the reflection mechanism

affects the thermal including mass transport of naturally convection Magnetohydrodynamic micropolar fluids flowing through a porosity vertically motion surface. The slip boundary by the sheet, which essentially states that a certain pressure field be proportionate to the fluid velocity, was initially proposed by Navier [31].

Further research into velocity profiles was justified by the many technological and academic uses involving flow across discs. Those experiments are all limited to border layers without slides. According to Beavers et al.[32] experimental results, slip acceleration does indeed occur at the porosity boundary sheet. Asghar et al.'s [33] investigation into the non-Newtonian flowing fluid resulting from oscillating a porous sheet. Spontaneous convection for magnetohydrodynamics through an infinitely long horizontal oscillation sheet having a stable amount of heat was investigated by Deka et al. [34]. Wu's [35] second-order slip concept was first studied. Iahak et al. [36] research focused on alternatives persistent motion or a stationary sheet with a micropolar liquid motion over it.

A comprehensive analysis for natural processes along with Hall impacts mostly towards electrically radiated hydromagnetic liquid dynamics passing more than a quasi-vertical barrier sheet was conducted by Pal et al. [37]. An iterative procedure was put out by Migun [38] to identify every characteristic for microscopic scraps inside this micropolar. The effect of slip limitation on electromagnetic peristaltic transport was addressed by Qayyum et al. [39] in relation to effects on heat production and electricity generation. Shehzad et al. [40] discussed the flow of micropolar treated water nanomaterial suspensions across a stretching surface. A micropolar fluid having consequent effects on temperature flow separation over a stretched surface by Ishak [41]. Sahoo, B [42] looked on Consequences like incomplete slip, entropy generation, and thermal radiation upon that heat exchange, as well as the Von Kármán circulation of a quasi-fluid that conducts electricity.

The objective of this investigation would be to examine the impact of a second-order slip boundary condition on the heat transfer of a micropolar fluid across a stretched surface and the MHD boundary layer flow. In the equation for energy, the influences of viscous dissipation are also reportedly. In an effort to turn the governing boundary layer equations into ODEs, similarity changes are put to use. After that, the equations are numerically explained with the help of MATLAB's built-in solver. The influence of significant factors has been investigated concerning the flow functions.

MATHEMATICAL ANALYSIS

Consider a micropolar fluid flowing steadily inside a laminar boundary layer through a stretched surface with a specific heat T_w and a second-order slip boundary condition. T_∞ describes the average ambient temperature. Let us take the surface, which is thought to be extending by a velocity of $u_w = ax$ .a stretched constant in which the circulation was subjected to either a strong horizontal magnetic field that was also continuously provided and was thought to still be maintained along the flow's favourable plane. Where a is stretched parameter. That stream was exposed to a strong $B = B_0$ horizontal magnetic field that is applied continuously and is considered to be perpendicular to the positive y-axis. Following boundary layer assumptions, the flow formulas are written as:

Industrial Engineering Journal
ISSN: 0970-2555
Volume : 52, Issue 10, No. 3, October : 2023

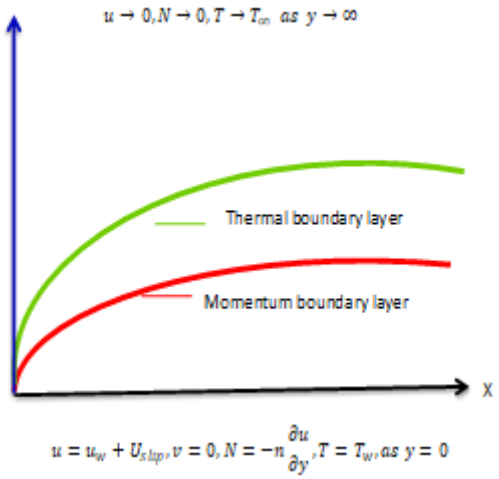

Figure 1: Flow geometry

Eq. of Continuity: $\frac{\partial u}{\partial x} + \frac{\partial v}{\partial y} = 0$ (1)

Eq. of Momentum: $u\frac{\partial u}{\partial x} + v\frac{\partial u}{\partial y} = \frac{(\mu+\kappa)}{\rho}\left(\frac{\partial^2 u}{\partial y^2}\right) + \frac{\kappa}{\rho}\frac{\partial N}{\partial y} - \frac{\sigma {B_0}^2}{\rho}u$ (2)

Eq. of Angular momentum: $u\frac{\partial N}{\partial x} + v\frac{\partial N}{\partial y} = \frac{\Omega}{j\rho}\frac{\partial^2 N}{\partial y^2} - \frac{k}{j\rho}\left(2N + \frac{\partial u}{\partial y}\right)$ (3)

Eq. of Energy: $u\frac{\partial T}{\partial x} + v\frac{\partial T}{\partial y} = \frac{\kappa}{\rho C_p}\left(\frac{\partial^2 T}{\partial y^2}\right)$ (4)

These are the circumstances at the boundary:

$$\left.\begin{aligned} u = u_w + U_{slip}, v = 0, N = -n\frac{\partial u}{\partial y}, T = T_w, \quad at\ y = 0 \\ u \to 0, \quad N \to 0, \quad T \to T_\infty, \qquad as \quad y \to \infty \end{aligned}\right\} \quad (5)$$

Wu's [139] slip velocity formula, that is applicable to each Knudsen number, Kn, and which utilised scientists like [43, 44, and 84], was provided as:

$$\mathrm{U_{slip}} = \frac{2}{3}\left(\frac{3-\alpha \mathrm{l}^2}{\alpha} - \frac{3}{2}\frac{1-\mathrm{l}^2}{\mathrm{K_n}}\right)\lambda\frac{\partial \mathrm{u}}{\partial \mathrm{y}} - \frac{1}{4}\left[\mathrm{l}^4 + \frac{2}{\mathrm{K_n^2}}(1-\mathrm{l}^2)\right]\lambda^2\frac{\partial^2 \mathrm{u}}{\partial \mathrm{y}^2}$$

$$\mathrm{U_{slip}} = \mathrm{A}\frac{\partial \mathrm{u}}{\partial \mathrm{y}} + \mathrm{B}\frac{\partial^2 \mathrm{u}}{\partial \mathrm{y}^2} \quad (6)$$

Here A and B are constant, $l = min\left[\frac{1}{K_n}, 1\right]$, we have $0 \le \alpha \le 1$. If $B < 0$, and hence the second term in the right-hand side of Eq. (6) is a positive number. $\gamma = A\sqrt{\frac{a}{v}}$, which is positive, $\delta = \frac{Ba}{v}$ is negative. $\Omega = \left(\mu + \frac{\kappa}{2}\right)j = \mu\left(1 + \frac{\beta}{2}\right)j$, where $\beta = \frac{\kappa}{\mu}$, such that $0 \le n \le 1$.

Measures of similarity are described as follows:

$$\eta = \left(\sqrt{\frac{a}{v}}\right)y \quad (7)$$

the nondimensional parameters are introduced

$$\left.\begin{aligned} f(\eta) = \frac{\varphi}{\sqrt{a\vartheta x}}, \quad g(\eta) = \frac{N}{ax\left(\sqrt{\frac{a}{v}}\right)}, \quad \theta(\eta) = \frac{T-T_\infty}{T_w-T_\infty} \end{aligned}\right\} \quad (8)$$

It's easy to see that Eq. (1) is always true in the context of Eqs. (1) -(4). In this case, the remaining equations are simplified to the following

$$(1+\beta)f''' + ff'' - (f')^2 + \beta g' - Mf' = 0 \quad (9)$$

$$\left(1 + \frac{\beta}{2}\right)g'' + fg' - gf' - \beta(2g + f'') = 0 \quad (10)$$

Industrial Engineering Journal
ISSN: 0970-2555
Volume : 52, Issue 10, No. 3, October : 2023

$$\theta'' + Prf\theta' = 0 \quad (11)$$

The transformed boundary conditions are

$$\left.\begin{array}{rl} f(0) = 0, f'(0) = 1 + \gamma f''(0) + \delta f'''(0), & \\ g(0) = -nf'''(0), \theta(0) = 1 & at \quad \eta = 0 \\ f'(\infty) \to 0, g(\infty) \to 0, \theta(\infty) \to 0, & as \quad \eta \to \infty \end{array}\right\} \quad (12)$$

Here prime denote the differentiation w.r.t to η and the non-dimensional parameters are introduced

$$M = \frac{\sigma B_0^2}{\rho a}, Pr = \frac{\nu}{\Lambda}, \beta = \frac{\kappa}{\mu}$$

Here local Nusselt number Nu_x may be defined as:

$$C_f = \frac{\tau_w}{\rho u_w^2} = \frac{(1+K)f''(0)}{\sqrt{Re_w}}, \mathrm{N}u_x = \frac{\mathrm{x}q_w(x)}{\mathrm{k}(T_w - T_\infty)} \quad (13)$$

The shear stress can be calculated by using the formula at the surface τ_w and the formula for determining the local surface heat flux transfer coefficient is wall heat flux q_w:

$$\tau_w = \left[(\mu + k)\left(\frac{\partial u}{\partial y}\right) + kN\right]_{y=0}, q_w(x) = -k_f \left(\frac{\partial T}{\partial y}\right)_{y=0} \quad (14)$$

By using the above equations, we get:

$$C_f \sqrt{\mathrm{Re}_x} = -\left(1 + \beta(1-n)\right) f''(0), \frac{Nu_x}{\sqrt{\mathrm{Re}_x}} = -\theta'(0) \quad (15)$$

METHOD OF SOLUTION

The set of connected ODEs (9) through (11) and the subsidiary boundary conditions (12) are solved by converting them into an initial value problem.

We set

$y_1 = f, y_2 = f', y_3 = f'', y_4 = g, y_5 = g', y_6 = \theta, y_7 = \theta', y_8 = \phi, y_9 = \phi'$ then the form below is used for nonlinear ODEs.

$$y'_3 = (\mathrm{M}^* y_2 + y_2 * y_2 - y_1 * y_2 - \beta * y_5) * (1/(1+\beta));$$

$$y'_5 = (y_2 * y_4 + \beta(2 * y_4 + y_3) - y_1 * y_5) * (1/(1 + \beta/2));$$

$$y'_7 = -(Pr * y_1 * y_7);$$

boundary limits are

$$\left.\begin{array}{c} y_1(0) = 0, y_2(0) = 1 + \gamma\, y_3(0) + \delta y'_3(0) \\ y_4(0) = -n y_3(0), y_6(0) = 1, \\ y_2(\infty) = 0, y_4(\infty) = ,0\ y_6(\infty) = 0. \end{array}\right\}$$

These resulting mathematical expressions can be integrated using MATLAB's built-in solver approach. All the above steps will be done again and again until the desired level 10^{-6} of accuracy

Results and discussion

The investigation into the research of micropolar fluid flow with suction/injection and viscous dissipation is being carried out. Using numerical methods, we have determined the velocity $f'(\zeta)$, stream velocity$f'(\zeta)$, angular velocity $g(\zeta)$, and temperature $\theta(\zeta)$ fields, as well as the skin friction factor and local Nusselt number, over a choice of values of the describing factors. This part determines to explore the varied physical properties that various embedding settings have on flow region profiles,

Industrial Engineering Journal
ISSN: 0970-2555
Volume : 52, Issue 10, No. 3, October : 2023

which are shown in the figures. Typical profiles of the dimensionless velocity, temperature, angular velocity, & concentration for diverse values of the material parameter β are revealed in Figures, accordingly. These f distribution curves are shown in Figures 2,3 and 4 along with the values of various constants such as the 1st slip ordered variable, the 2nd slip ordered variable δ, and the material variable. The images show that thickness of the border grows in the process of values of γ, but also δ, going up, but it becomes reduced when the quantity of β goes up.

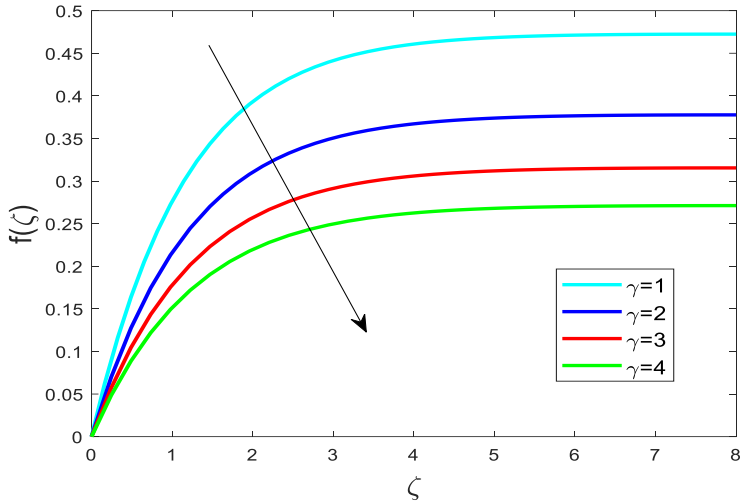

Figure2: f (ζ) v/s γ with β = 2, M = 1, n = 0.5, δ = −1, Pr =1.

These f distribution curves are shown in Figure 2 along with the values of various constants such as the 1st order slip parameter γ. According to the picture, As values of γ rises.

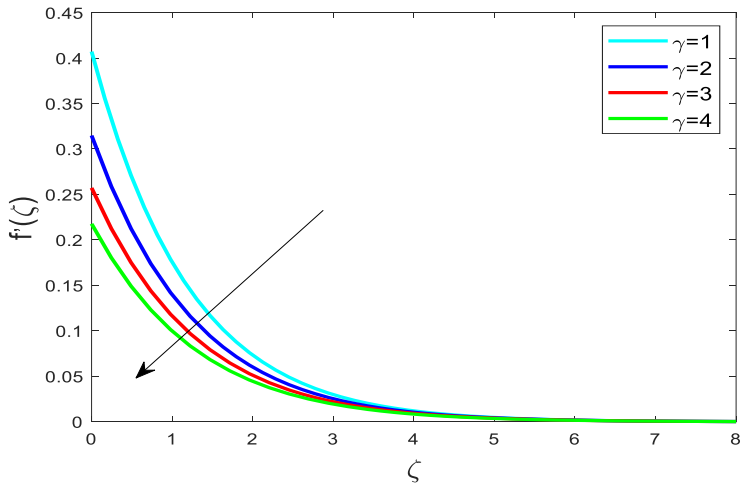

Figure3: $f'(\zeta)$ v/s γ, if δ = −1, M = 1, n = 0.5, Pr =1, β = 2.

Figure 3 depicts a non-geometric velocity distribution graph with the first order slip factor f ′ (η) varying priorities. The above graph demonstrates that, in particular, the function f ′ (η) has a diminishing significance as the number γ increases.

Industrial Engineering Journal
ISSN: 0970-2555
Volume : 52, Issue 10, No. 3, October : 2023

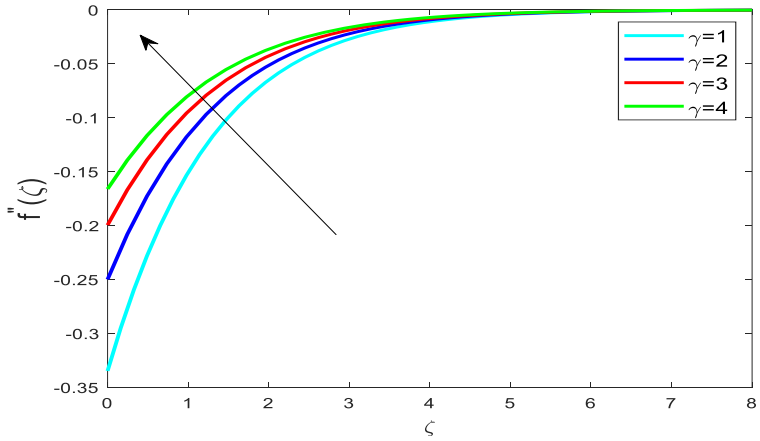

Figure 4: f ″(ζ) v/s γ if δ = −1, β = 2, n = 0.5, M = 1, Pr =1.

Figure 4 depicts rises the first order slip factor f ″(η) also rises.

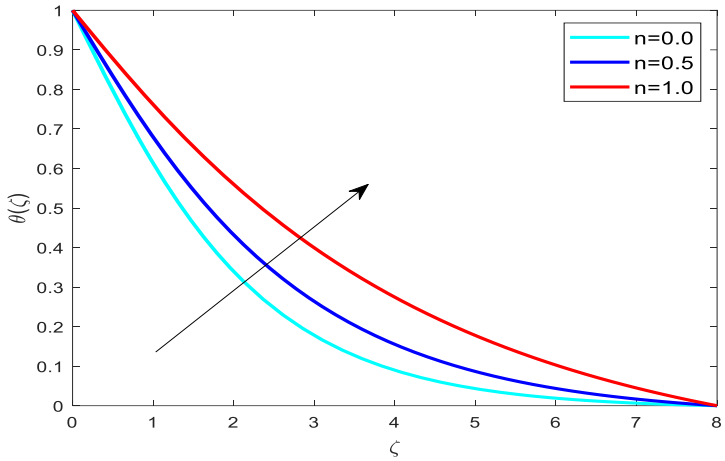

Figure 5 : θ(ζ) v/s n with Pr =1, δ = −1, β = 2, γ =1, M = 1 .

An influence of the similarity parameter n towards temperature distribution is illustrated in Figure 5. The graphic enables us to see such a rising curve as the similarity factor corresponds to a temperature rise.

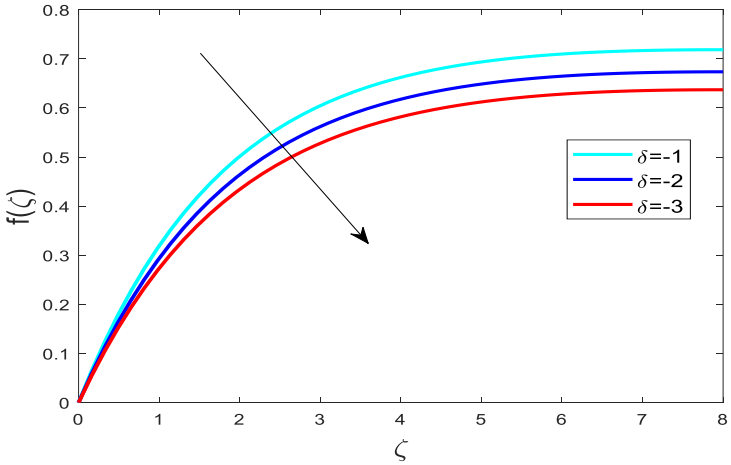

Figure 6: f(ζ) v/s δ if Pr =1, β = 2, γ =1, M = 1 , n = 0.5.

These f distribution curves are shown in Figures 6, along with the values of various constants such as the 2nd order slip parameter δ. As values of δ rises.

Industrial Engineering Journal
ISSN: 0970-2555
Volume : 52, Issue 10, No. 3, October : 2023

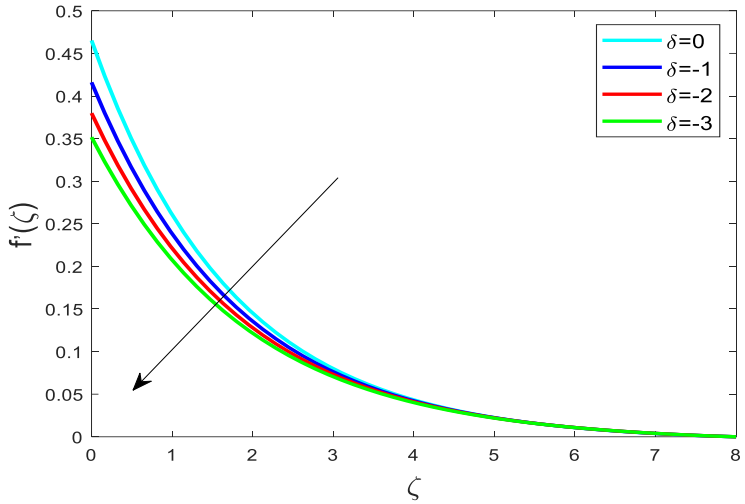

Figure 7: $f'(\zeta)$ v/s δ if γ =1, M = 1 , β = 2, n = 0.5, Pr =1.

Figure 7 depicts a non-geometric velocity distribution graph with the 2nd order slip factor f ′ (η) varying priorities. The above graph demonstrates that, in particular, the function f ′ (η) has a diminishing significance as the number δ increases.

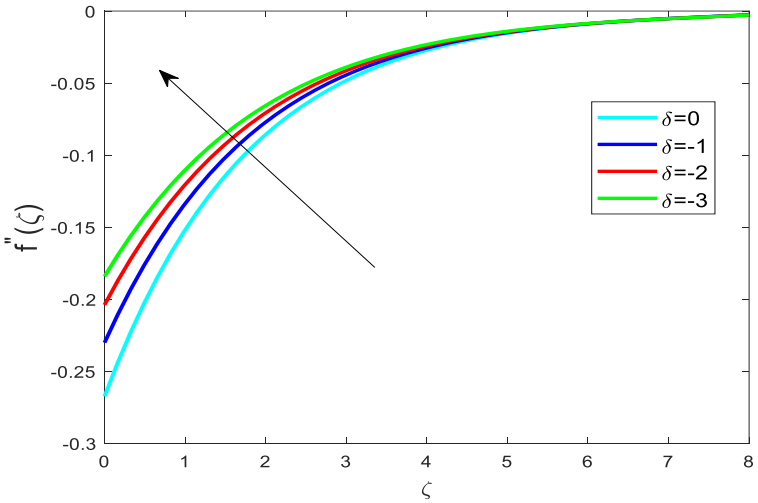

Figure 8: f ″(ζ) v/s δ if M = 1 ,n = 0.5, Pr =1, γ =1, β = 2.

Figure 8 depicts a non-geometric rises the second order slip factor also grow up.

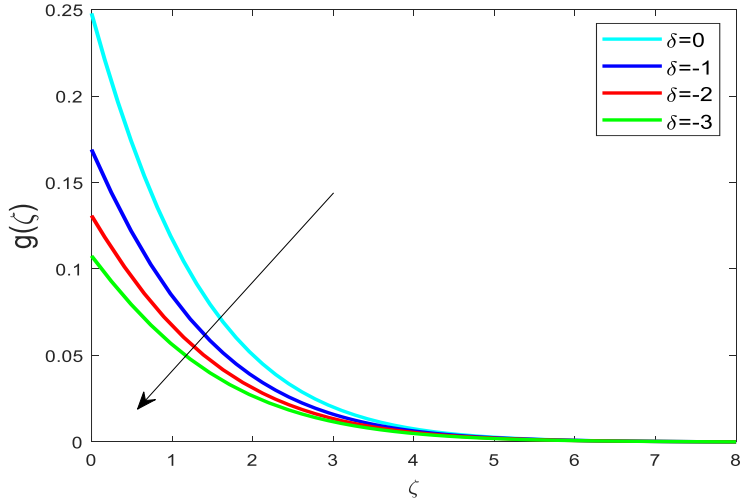

Figure9: g(ζ) v/s δ if γ =1,n = 0.5, M = 1 , Pr =1, β = 2.

Industrial Engineering Journal
ISSN: 0970-2555
Volume : 52, Issue 10, No. 3, October : 2023

The curves of the angular velocity profiles along with second-order slip factor shown in fig 9. According to what can be seen from the figure, the depth of the microrotation boundary layer reduces as the numbers about the second-order slip factor grow.

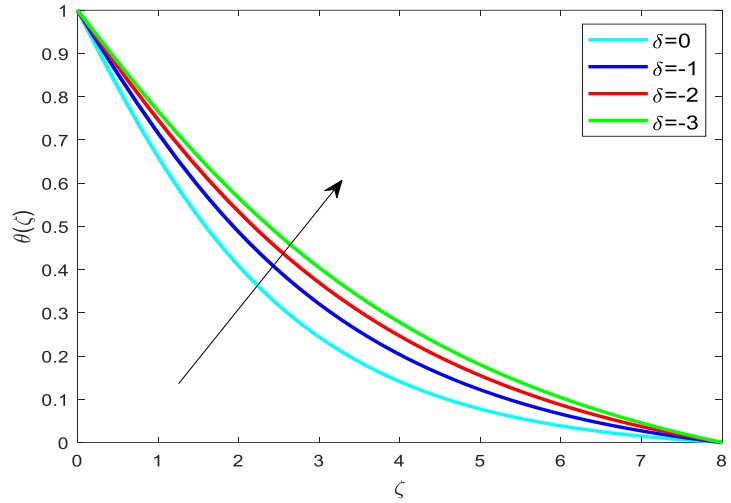

Figure 10: $\theta(\zeta)$ v/s δ if M = 1, n = 0.5, Pr =1, β = 2, γ =1.

Figure 10 shows the overall temperature distribution as a function of the impacts of the second-order slip factor. If a flow field's temperature is a real variable, it goes up when the slip variable for the second order is increased.

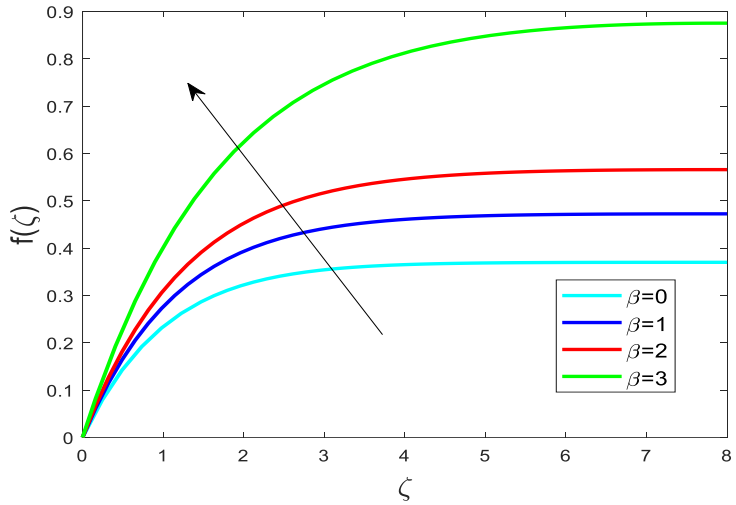

Figure 11: f (ζ) v/s β if Pr =1, $\delta = -1$, M = 1, n = 0.5, γ =1.

This set of distribution curves is shown in Figure 11 along with the values of various constants such as the material parameter. According to the pictures, the depth of the boundary layer grows in the process of values but it becomes reduced when the quantity of β goes up.

Industrial Engineering Journal
ISSN: 0970-2555
Volume : 52, Issue 10, No. 3, October : 2023

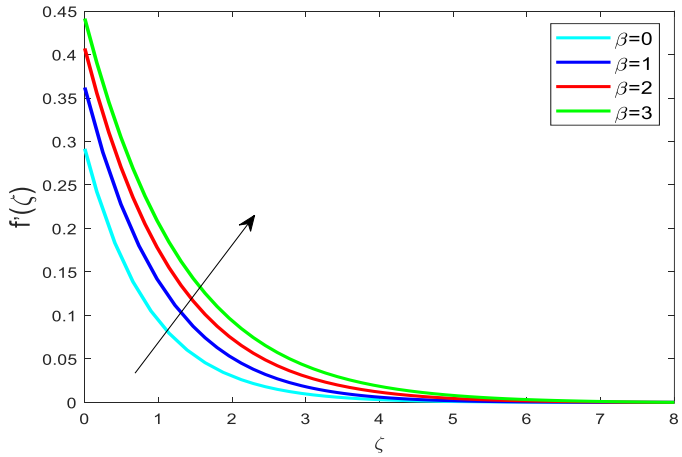

Figure 12: $f'(\zeta)$ v/s β if $\delta=-1$, M = 1, γ =1, Pr =1, n = 0.5.

Its non-geometric velocity distribution curve, denoted either by the symbol $f'(\zeta)$, is shown in Figure 12 for a selection of different quantities of β. Figure 12 shows how the number of $f'(\zeta)$ rises when β is increased to higher and higher levels.

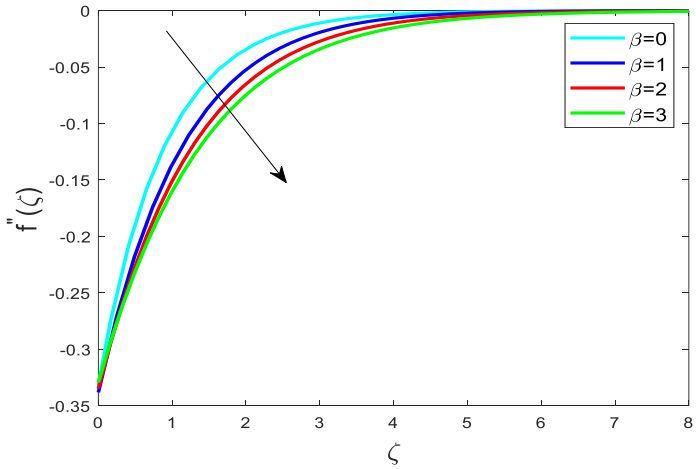

Figure13: $f''(\zeta)$ v/s β if n = 0.5, γ =1, $\delta=-1$, Pr =1, M = 1.

An influence of material factor on $f''(\zeta)$ is illustrated in Image 13 that it increases as a consequence of actual values for a material parameter. With this added, the overall depth of the boundary layer around a coefficient of skin friction rises, as does the value of the material parameter β.

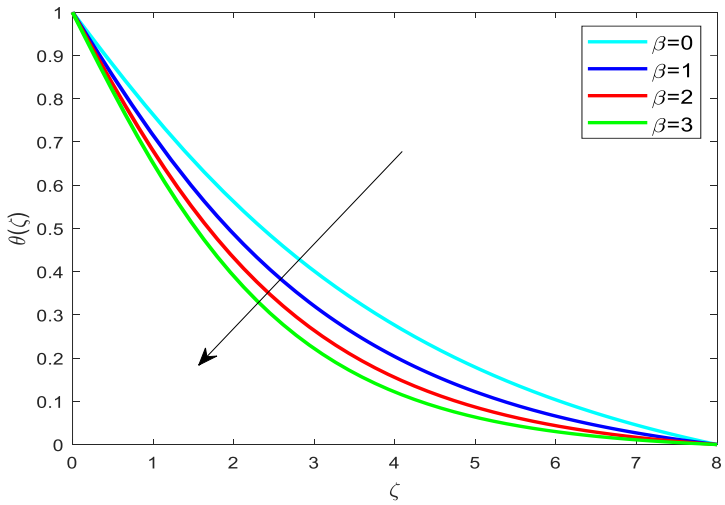

Figure 14: $\theta(\zeta)$ v/s β when M = 1, γ =1, Pr =1, n = 0.5, $\delta=-1$.

Industrial Engineering Journal
ISSN: 0970-2555
Volume : 52, Issue 10, No. 3, October : 2023

The effects of the material parameter β on temperature profile are given in Figs. 14. From the figure, We are able to see that there is a negative relationship between the material parameter β and the temperature of a fluid flow.

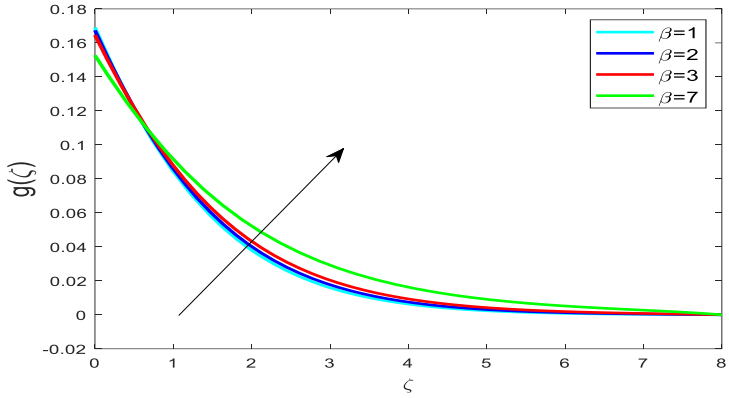

Figure 15: $g(\zeta)$ v/s β if $\delta=-1$, n = 0.5, Pr =1, M = 1, γ =1

The curve of the angular velocity distribution since the material parameter is depicted in Figure 15. Moreover, as illustrated in Figure 15, the depth of the angular velocity boundary layer grows as the value of the material parameter β rises.

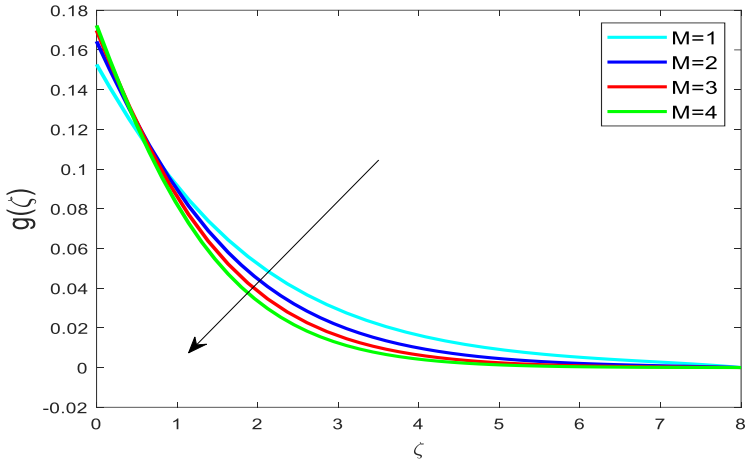

Figure 16: $g(\zeta)$ v/s M if Pr =1, γ =1, n = 0.5, $\delta=-1$.

The curve of the angular velocity distribution since the natural parameter is depicted in Figure 16. According to the figure, the depth of a microrotation boundary layer becomes reduced whenever there is a rise inside the numbers as regards the magnetic parameter M.

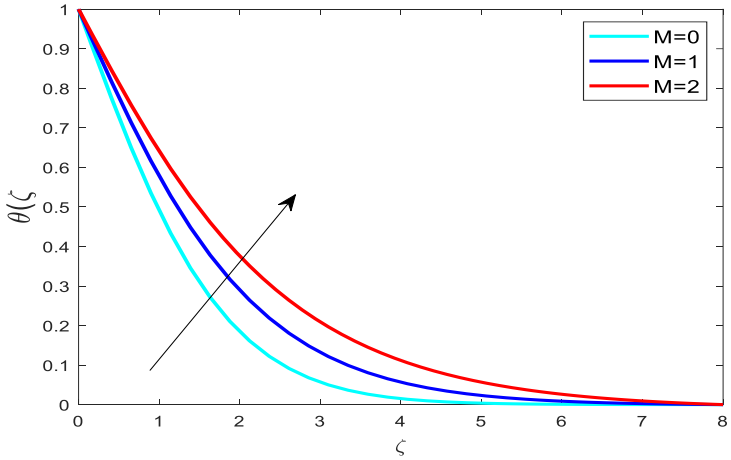

Figure 17: $\theta(\zeta)$ v/s M if $\delta=-1$, Pr =1, n = 0.5, γ =1.

Industrial Engineering Journal
ISSN: 0970-2555
Volume : 52, Issue 10, No. 3, October : 2023

An influence that the magnetic parameter M has on the temperature distribution is shown in Figures 17. It is indeed clear by looking just at the curve that the temperature of fluid flow increases when the magnetic parameter M was increased.

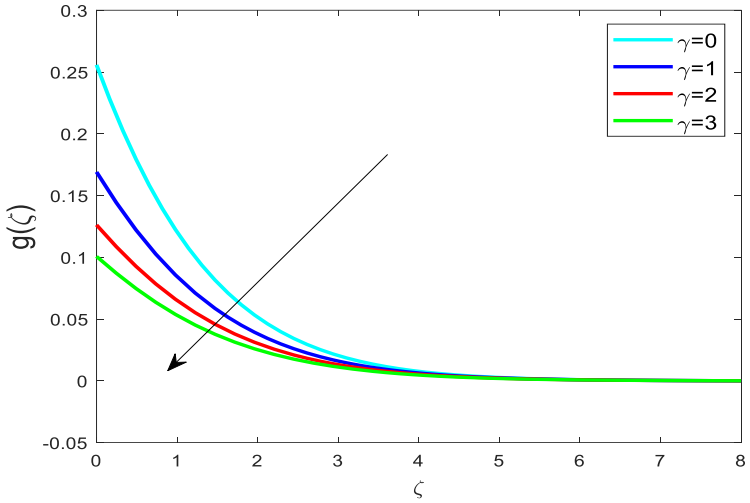

Figure 18: $g(\zeta)$ v/s γ if n = 0.5, $\delta = -1$, M = 1, β =1, Pr =1.

The curve of the angular velocity distribution since the 1st slip ordered parameter is depicted in Figure 18 illustrates the relationship between the rising 1st slip ordered factor along with the decreasing depth of the microrotation boundary layer. By addition to this, when the first order slip parameter k is increased, the angular velocity measured just by surface drops. In some kind of comparable way, clearly illustrated in Figure 18, the depth of the angular velocity boundary layer reduces when the magnetic parameter M is increased. Table 1 compares $-\theta'(0)$ for a variety of Pr quantities while and absence are kept at M, λ,δrespectively. Table 2 Such statistical analysis based on the coefficient of skin friction$-f''(0)$ current this study considering varying parameters γ while M = 0,$\delta = 0$ and lie in good accuracy with previous being included in [42].Table 3 illustrate the skin friction, rises for M and falls down for γ, δ and local Nusselt number goes down with enhanced values of γ, δ, β .

Table 1: Comparing the local Nusselt number for $-\theta'(0)$when $n = 0.5, M = 0.0, \beta = 0.0$, for varying parameters Pr by an earlier finding.

Pr	**Previous results Ishak [41]**	**Present result $-\theta'(0)$**
0.72	0.4631	0.464984
1.0	0.5820	0.582190
3.0	1.1652	1.165140
10.0	2.3080	2.307872
100.0	7.7657	7.765213

Table 2: Results Comparing for $-f''(0)$ for the slip parameter when M = 0, δ=0.

γ	**Previous results Sahoo, B [42]**	**Present results $-f''(0)$**
0.0	1.001154	1.000063
0.1	0.871447	0.872151
0.2	0.774933	0.776450
0.3	0.699738	0.701626

0.5	0.589195	0.591279
1.0	0.428450	0.430253
2.0	0.282893	0.284081
3.0	0.213314	0.214157
5.0	0.144430	0.144940
10.0	0.081091	0.081329
20.0	0.043748	0.043678

Table 3: values of skin friction coefficient $-f''(0)$ and local Nusselt number$-\theta'(0)$ for a variety of diverse Pr = 1, n = 0.5 other factors are M, β & δ

M	$\boldsymbol{\beta}$	$\boldsymbol{\delta}$	$\boldsymbol{-f''(0)}$			$\boldsymbol{-\theta'(0)}$		
			γ=1	**γ =2**	**γ =3**	**γ =1**	**γ =2**	**γ =3**
0.1	0.1	-1	0.322013	0.239887	0.191365	0.381550	0.343217	0.316653
0.2	0.1	-1	0.326222	0.243369	0.194262	0.360267	0.321399	0.294671
0.3	0.1	-1	0.329316	0.245935	0.196380	0.341089	0.302407	0.276109
0.4	0.1	-1	0.331505	0.247778	0.197900	0.323882	0.285928	0.260462
0.2	1	-1	0.317331	0.237082	0.189600	0.406605	0.362291	0.331530
0.2	2	-1	0.306805	0.230139	0.184635	0.443077	0.395403	0.362007
0.2	3	-1	0.297123	0.223900	0.180228	0.470263	0.420621	0.385592
0.2	4	-1	0.288416	0.218349	0.176326	0.491531	0.440671	0.404564
0.2	2	-1	0.306805	0.230139	0.184635	0.443077	0.395403	0.362007
0.2	2	-2	0.258813	0.203904	0.168276	0.414309	0.376721	0.348749
0.2	2	-3	0.226213	0.184123	0.155138	0.392698	0.361603	0.337526

Conclusions

These impacts of second-order slip factor flow, along with boundary layer flow and a magnetic field, include the transport of heat in a micropolar across a stretched surface, have been examined but also addressed in this research study. Through the use of the approximation transformation, the boundary layer problems that regulate the flow issue were transformed into ODEs. After that, the system of equations that were acquired were calculated, and the results were obtained by utilising the bvp4c programme that comes with the MATLAB program. The impacts of several regulating factors, Slip qualities include like γ and β. magnetic parameter M, Prandtl-Number P r, and the material parameter β, were explained utilising diagrams and tables. These impacts may be seen in the formulas for momentum, energy, and microrotation.

According to research findings, the slip parameter, and the material parameter both have a significant impact on a particular flow velocity, along with the skin friction coefficient. Furthermore, the depth of either the slip characteristics increases in proportion to the actual numbers of border surface velocity. So, when the numbers associated with two slip variables continue to go up, the overall depth of a thermal boundary layer also keeps going up. Additionally, the friction of the skin.

REFERENCES

[1]. C.L.M.H. Navier, Sur les lois du mouvement des fluids, Men. Acad. R. Sci. Inst. Fr 6 (1827) 389e440.
[2]. H.I. Andersson, Slip flow past a stretching surface, Acta Mech. 158 (2002) 121-125.
[3]. T. Fang, J. Zhang, and S. Yao, "Slip MHD viscous flow over a stretching sheet – An exact solution," Commun. Nonlinear Sci. Numer. Simulat., vol. 14, pp. 3731-3737, 2009.

[4]. K. Bhattacharyya, S. Mukhopadhyay, and G. C. Layek, "Slip effects on unsteady boundary layer stagnation-point flow and heat transfer towards a stretching sheet," Chin. Phys. Lett., vol. 28, Art. No 094702, 2011.
[5]. Ahmad, Saeed, Muhammad Yousaf, Amir Khan, and Gul Zaman. "Magnetohydrodynamic fluid flow and heat transfer over a shrinking sheet under the influence of thermal slip." Heliyon 4, no. 10 (2018): e00828. https://doi.org/10.1016/j.heliyon.2018.e00828.
[6]. Yang, Weidong, Xuehui Chen, Zeyi Jiang, Xinru Zhang, and Liancun Zheng. "Effect of slip boundary condition on flow and heat transfer of a double fractional Maxwell fluid." Chinese Journal of Physics 68 (2020): 214- 223.https://doi.org/10.1016/j.cjph.2020.09.003.
[7]. B. Sahoo, S. Poncet, Flow and heat transfer of a third grade fluid past an exponentially stretching sheet with partial slip boundary condition, Int. J. Heat Mass Trans. 54 (2011) 5010-5019.
[8]. K. Das, Slip flow and convective heat transfer of nanofluids over a permeable stretching surface, Computers & fluids, Vol. 64, 2012, pp. 34-42.
[9]. A Majeed, FM Noori, A Zeeshan, T Mahmood, SU Rehman and I Khan. Analysis of activation energy in magnetohydrodynamic flow with chemical reaction and second order momentum slip model. Case Stud. Therm. Eng. 2018; 12, 765-73.
[10]. G. Singh, A.J. Chamkha, Dual solutions for second-order slip flow and heat transfer on a vertical permeable shrinking sheet, Ain Shams Eng. J. 4 (2013) 911–917.
[11].A.V. Rosca, I. Pop, Flow and heat transfer over a vertical permeable stretching/ shrinking sheet with a second-order slip, Int. J. Heat Mass Transf. 60 (2013) 355–364.
[12]. Turkyilmazoglu M. Analytic heat and mass transfer of the mixed hydrodynamic/thermal slip MHD viscous flow over a stretching sheet. Int J Mech Sci 2011; 53:886–96.
[13]. Zhang T, Jia L, Wang Z. Validation of Navier-Stokes equations for slip flow analysis within transition region. Int J Heat Mass Transf 2008; 51:6323–7.
[14]. G.C. Pereira, Effect of variable slip boundary conditions on the flows of pressure driven non-Newtonian fluids, J. Non-Newtonian Fluid Mech. 157 (2009) 197-206.
[15]. F.T. Akyildiz, H. Bellout, K. Vajravelu, R.A. Van Gorder, Existence results for third order nonlinear boundary value problems arising in nano boundary layer fluid flows over stretching surfaces, Nonlinear Anal. Real World Appl. 12 (2011) 2919e2930.
[16]. M.H. Yazdi, S. Abdullah, I. Hashim, M.N. Zulkifli, A. Zaharim, K. Sopian, Convective heat transfer of slip liquid flow past horizontal surface within the porous media at constant boundary conditions, in: Recent Advances in Applied Mathematics (Ed. Stephen Lagakos et. al.), WSEAS Press, USA, 2010 527–534.
[17]. P.A. Thompson, S.M. Troian, A general boundary condition for liquid flow at solid surfaces, Nature 389 (1997) 360–362.
[18]. Noghrehabadi A, Pourrajab R, Ghalambaz M. Effect of partial slip boundary condition on the flow and heat transfer of nanofluids past stretching sheet prescribed constant wall temperature. International Journal of Thermal Sciences. 2012; 54:253–261.
[19]. Nandeppanavar MM, Vajravelu K, Abel MS, Siddalingappa M. Second order slip flow and heat transfer over a stretching sheet with non-linear Navier boundary condition. International Journal of Thermal Sciences. 2012; 58:143–150.
[20]. Chauhan DS, Olkha A (2011) Slip flow and heat transfer of a second-grade fluid in a porous medium over a stretching sheet with power-law surface temperature or heat flux. Chem Eng. Commun 198:1129–1145.
[21] Aziz, A,Fang,T: Viscous flow with second-order slip velocity over a stretching sheet. Z. Naturforsch. 65a, 1087–1092 (2010).
[22]. Qasim, M., Hayat, T., Hendi, A.A.: Effects of slip conditions on stretching flow with ohmic dissipation and thermal radiation. Heat Transf. Asian Res. 40, 641–654 (2011).
[23]. Saidulu, B. " Role of Magnetic Field on Natural Convective Towards a Semi-Infinite Vertically Inclined Plate in Presence of Hall Current with Numerical Solutions: A Finite Difference Technique

", International Journal of Scientific and Innovative Mathematical Research, vol. 6, no. 2, p. 25-40, 2018., http://dx.doi.org/10.20431/2347-3142.0602003.

[24]. Saidulu, B., and Reddy, K. S.: Evaluation of combined heat and mass transfer in hydromagnetic micropolar flow along a stretching sheet when viscous dissipation and chemical reaction is present. Partial Differential Equations in Applied Mathematics, 2023, 7, 100467. https://doi.org/10.1016/j.padiff.2022.100467.

[25] Saidulu B, Reddy KS. Comprehensive analysis of radiation impact on the transfer of heat and mass micropolar MHD free convective fluid flow across a stretching permeability sheet with suction/injection. Heat Transfer. 2023;1-16.doi:10.1002/htj.22829.

[26] M. A. Hossain and H. S. Takhar, "Radiation Effect on Mixed Convection along a Vertical Plate with Uniform Surface Temperature," Heat Mass Transfer, Vol. 31, No. 4, 1996, pp. 243-248. doi:10.1007/BF02328616.

[27] A. Pantokratoras, "Study of MHD Boundary Layer Flow over a Heated Stretching Sheet with Variable Viscosity: A Numerical Reinvestigation," International Journal of Heat and Mass Transfer, Vol. 51, No. 1-2, 2008, pp. 104- 110. doi:10.1016/j.ijheatmasstransfer.2007.04.007.

[28] Kalaivanan R, Renuka P, Ganesh NV, Hakeem AKA, Ganga B, Saranya S. Effects of aligned magnetic field on slip flow of Casson fluid over a stretching sheet. Procedia Eng. 2015;127:531-538.

[29] Fang T, Zhang J, Yao S. Slip MHD viscous flow over a stretching sheet-an exact solution. Commun Nonlin Sci Numer Simulat 2009;14:3731–373.

[30] Bakr AA. Effects of chemical reaction on MHD free convection and mass transfer flow of a micropolar fluid with oscillatory plate velocity and constant heat source in a rotating frame of reference. Comm Nonlinear Sci Numer Simul. 2011;1(16):698-710.

[31] Navier CLMH. Memoire Surles du Movement desMem. Acad R Sci Inst Fr. 1823;6:389.

[32] Beavers GS, Joseph DD. Boundary conditions at a naturally permeable wall. J Fluid Mech 1967;30:197–207.

[33] Asghar S, Mohyuddin MR, Hayat T, Siddiqui AM. The flow of a non-Newtonian fluid induced due to the oscillations of a porous plate. Math Probl Eng. 2004;2:133-143.

[34] Deka RK, Das UN, Soundalgekar VM. Free convection effects on MHD flow past an infinite vertical oscillating plate with constant heat flux. Indian J Math. 1997; 39:195-202.

[35] Wu L. A slip model for rarefied gas flows at arbitrary Knudsen number. Appl Phys Lett. 2008;93:253103. https://doi.org/10.1063/1.3052923.

[36] Iahak A, Nazar R, Pop I. Boundary-layer flow of a micropolar fluid on a continuous moving or fixed surface. Can J Phys. 2006;84(5):399-410.

[37] D. Pal, B. Talukdar, I. S. Shivakumara, K. Vajravelu, Effects of hall current and chemical reaction on oscillatory mixed convection-radiation of a micropolar fluid in a rotating system, Chem. Eng. Commun. 199(2012), 943– 965.

[38] N.P. Migun, Experimental method of determining parameters characterizing the microstructure of micropolar liquids, J. Eng. Phy. 41(1981), 832–835.

[39] S. Qayyum, M.I. Khan, W. Chamam, W.A. Khan, Z. Ali, W. Ul-Haq, Modeling and theoretical investigation of curved parabolized surface of second-order velocity slip flow: combined analysis of entropy generation and activation energy, Mod. Phys. Lett. B (2020) 2050383.

[40] S.A. Shehzad, M.G. Reddy, P. VIjayakumari, I. Tlili, Behavior of ferromagnetic Fe2SO4 and titanium alloy Ti6Al4v nanoparticles in micropolar fluid flow, Int. Commun. Heat Mass Transf. 117 (Oct 2020) 104769, https://doi.org/10.1016/j. icheatmasstransfer.2020.104769.

[41] Ishak A (2010) Thermal boundary layer flow over a stretching sheet in micropolar fluid with radiation effect. Meccanica 45:367–373.

[42] Sahoo, B. (2009). Effects of partial slip, viscous dissipation and Joule heating on Von Kármán flow and heat transfer of an electrically conducting non-Newtonian fluid. Communications in Nonlinear Science and Numerical Simulation, 14(7), 2982-2998.